

## 铝合金飞秒激光单步法和三步法旋切打孔技术研究

任云鹏<sup>1\*</sup>, 程力<sup>1</sup>, 周王凡<sup>1</sup>, 陈燕<sup>2</sup>, 何坤<sup>1</sup>, 涂新诚<sup>1</sup>, 叶云霞<sup>1</sup>, 任乃飞<sup>1</sup><sup>1</sup>江苏大学机械工程学院, 江苏 镇江 212013;<sup>2</sup>江苏大学材料科学与工程学院, 江苏 镇江 212013

**摘要** 铝合金由于其优良的物理化学性能,在工业生产中得到了广泛应用,但铝合金的高反射率和高热导率限制了激光加工技术在铝合金精密加工中的应用。采用控制变量法研究了铝合金单步法旋切打孔技术中的激光重复频率、扫描次数、扫描速度、进给次数对微孔进出口形貌和锥度的影响规律。针对铝合金单步法旋切打孔中存在的锥度大和进出口形貌差等问题,提出了三步法旋切打孔方法。结果表明,该方法可以有效地减小微孔的锥度,改善进出口形貌,减少孔口周围的飞溅物堆积。主要原因是该方法可以有效地促进打孔过程中熔渣和等离子体的排出,减少其对激光能量的扰动,提高了激光能量的稳定性和均匀性。

**关键词** 激光技术; 飞秒激光; 旋切打孔; 铝合金; 锥度

中图分类号 TN249

文献标志码 A

DOI: 10.3788/CJL202249.2202020

## 1 引言

随着现代工业的迅速发展,人们对高品质微米级小孔的应用需求<sup>[1-8]</sup>越来越多,各领域对微孔进出口形貌和锥度均有严格的要求。铝合金因密度低、比强度高、铸造性能好、抗腐蚀性能优良等优点<sup>[9-10]</sup>,被广泛应用于汽车、轨道交通<sup>[11-14]</sup>、航天航空<sup>[15-16]</sup>、化工<sup>[17]</sup>、半导体<sup>[18]</sup>等重要产业中。

常见的铝合金微孔加工技术,如电火花加工<sup>[19]</sup>和离子束加工<sup>[20]</sup>等,存在加工效率低、锥度大、成本高等问题。激光打孔技术<sup>[21-24]</sup>相比于其他微孔加工工艺,具有加工精度和效率高、柔性好、无工具损耗等优势<sup>[25-26]</sup>。但铝合金材料中存在高密度自由电子,对激光具有高反射率<sup>[27-28]</sup>和高热导率<sup>[29]</sup>,容易造成孔周形貌差、锥度大等问题,严重影响器件的使用性能。

国内外学者针对铝合金激光打孔进行了广泛的研究。Krstulović 等<sup>[30]</sup>比较了空气和不同厚度水层下铝合金的激光打孔结果,发现在水层的约束下,材料的去除效率得到有效提高,飞溅物在进出口的沉积减少,小孔质量得到明显改善。钱晓忠等<sup>[31]</sup>采用控制变量法研究了扩束比、辅助气体气压和脉冲能量等参数对 5052 铝合金激光打孔质量的影响规律。Tunna 等<sup>[28]</sup>研究了单脉冲能量、波长和光斑直径对单脉冲的平均蚀刻深度、微孔孔周形貌和截面锥度的影响。Ahn 等<sup>[32]</sup>通过数值分析与试验对比,定量分析了脉冲宽度和重复频率对 1050 铝合金薄板上微孔入口直径、形

状、锥角和微孔附近温度分布的影响,从而得到最佳打孔参数。Zhao 等<sup>[33]</sup>使用超快激光对铝合金等四种金属材料进行了打孔试验研究,分析了脉冲个数和脉冲能量对微孔进出口形貌、孔深及孔壁质量的影响,通过研究四种材料的烧蚀阈值与热物理性质对微孔尺寸的影响,发现材料的烧蚀阈值与孔深呈反比关系,即对于烧蚀阈值较高的金属材料,相同激光工艺参数下加工的孔深较小,反之孔深较大。张学谦等<sup>[23]</sup>使用飞秒激光旋切打孔技术加工了带有热障涂层的高温合金的气膜孔,通过对重铸层以及微孔入口处附着物的分析,证明了材料去除机理是材料通过液相爆破的方式以纳米颗粒的形式快速离开基体。

本文采用控制变量法研究了旋切打孔中激光重复频率、扫描次数、扫描速度、进给次数对微孔进出口形貌和锥度的影响规律。针对铝合金材料激光打孔中存在的锥度大、进出口形貌差等问题,对现有旋切工艺进行了改进,提出了三步法旋切打孔工艺。通过对微孔锥度和表面飞溅物的分析,揭示了三步法旋切打孔工艺的改善机制。结果表明,该方法可以有效地减小微孔的锥度,改善微孔进出口形貌,减少孔口周围飞溅物的堆积。

## 2 试验设备与方法

本文使用的激光加工设备为飞秒光纤激光器,其主要性能参数如表 1 所示。图 1 为激光加工系统的光路图,飞秒(FS)激光器产生的光束经扩束镜扩束后,

收稿日期: 2022-04-24; 修回日期: 2022-05-17; 录用日期: 2022-06-09

基金项目: 中国博士后科学基金(2020M671409)、江苏省博士后科学基金(2020Z030)

通信作者: \*renyp@ujs.edu.cn

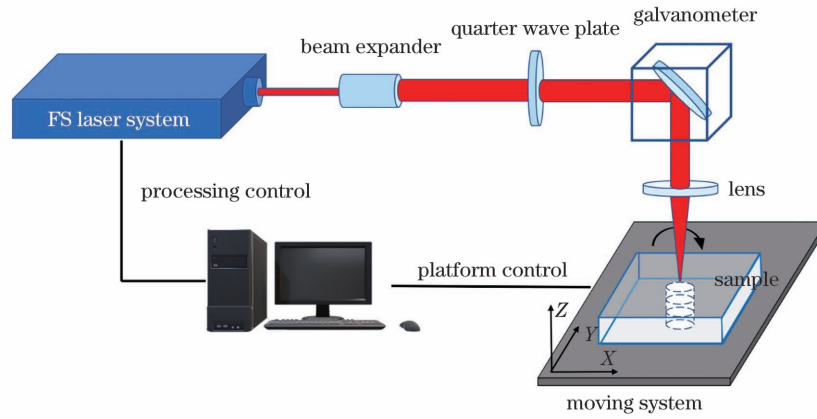


图 1 激光加工光路示意图

Fig. 1 Schematic of laser processing optical path

表 1 飞秒光纤激光器的主要参数

Table 1 Main parameters of femtosecond fiber laser

Parameter	Power	Wavelength	Pulse duration	Frequency	Maximum pulse energy	Focus spot diameter	Beam quality	Beam mode
Content	80 W	1030 nm	270 fs-10 ps	50 kHz-19 MHz	160 $\mu$ J	30 $\mu$ m	$M^2 < 1.3$	TE <sub>00</sub> Gaussian mode

进入扫描振镜并经场镜聚焦后在 X-Y 平面上运动,在 Z 轴方向上步进电机在电荷耦合元件(CCD)相机的引导下将聚焦光束的束腰位置定位在样品表面上。本文所用的试验材料为 1 mm 厚的 1060 铝合金,在其上加

工直径为 200  $\mu$ m 的微孔。1060 铝合金的化学成分如表 2 所示,使用碳化硅砂纸对线切割成型的样品表面进行打磨,并在乙醇溶液中超声振动 10 min 以清洗样品,保证材料表面的平整度和洁净度。

表 2 1060 铝合金的化学成分

Table 2 Chemical compositions of 1060 aluminum alloy

Chemical composition	Zn	Ti	V	Mn	Si	Fe	Cu	Mg	Al
Mass fraction /%	0.05	0.03	0.05	0.03	0.25	0.35	0.05	0.03	Bal.

本文在常规单步法旋切打孔工艺的基础上,提出了一种新的打孔方法,即三步法旋切打孔。图 2(a)为单步法旋切打孔的扫描路径示意图,激光束聚焦于最内圈(C1),沿顺时针方向逐层向最外圈(C9)递进扫描,加工完一层后,向下进给一定的距离。重复上述 C1~C9 的加工过程,直至形成贯穿的微孔。图 2(b)为三步法旋切打孔的扫描路径示意图,将 C1~C9 由内向外每三圈设置为一个圆环。采用三步法旋切打孔时,激光束聚焦于最内圈 C1 并沿顺时针方向向第一圆环的外圈(C3)递进扫描,在纵向上采用与单步法旋

切打孔工艺相同的进给方式完成第一圆环的加工。第一圆环加工完成后,在铝合金板上获得了一个孔径小于目标尺寸的中心孔。随后激光聚焦于 C4 圈和 C7 圈,以相同的方式完成第二、三圆环的加工。单步法和三步法旋切打孔的加工原理分别如图 3(a)、(b)所示。在单步法旋切打孔过程中,激光束聚焦于材料上表面进行烧蚀加工并逐层向下移动,直至击穿材料形成微孔。三步法旋切打孔过程分为三个阶段,首先利用第一圆环在微孔中心将材料击穿,形成预制孔洞,然后利用第二圆环拓宽孔径,最后利用第三圆环修饰孔形。

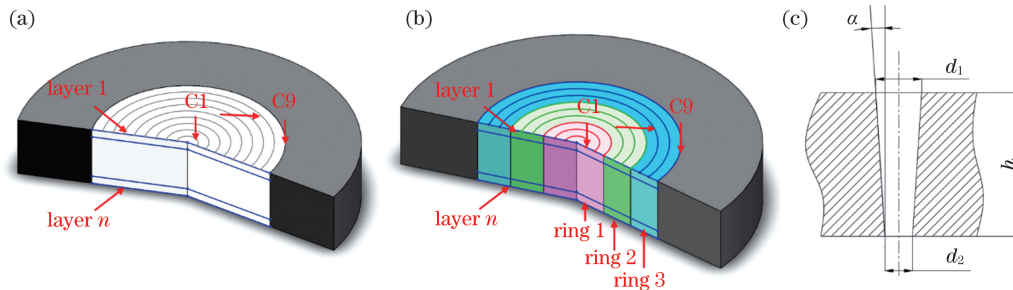


图 2 激光扫描路径和锥度测量方法示意图。(a)单步法旋切打孔;(b)三步法旋切打孔;(c)锥度测量方法

Fig. 2 Schematics of laser scanning path and taper measurement method. (a) Single-step trepanning drilling; (b) three-step trepanning drilling; (c) taper measurement method

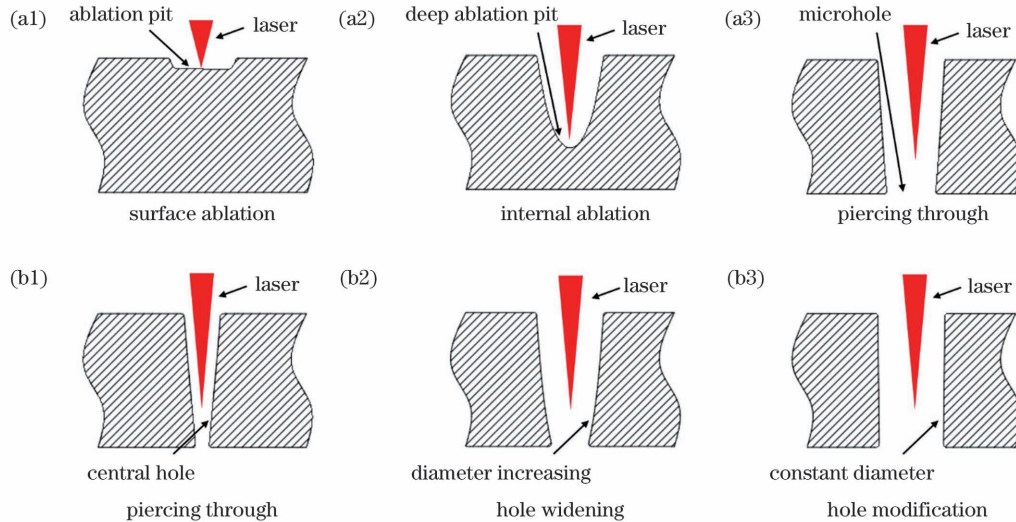


图 3 激光旋切打孔法的原理示意图。(a1)~(a3)单步法旋切打孔;(b1)~(b3)三步法旋切打孔

Fig. 3 Schematics of laser trepanning drilling method. (a1)~(a3) Single-step trepanning drilling; (b1)~(b3) three-step trepanning drilling

本文通过控制变量法研究了微孔出入口形貌及锥度随脉冲重复频率、扫描次数、进给次数、扫描速度的变化规律,并在最优参数下对比了单步法与三步法旋切打孔工艺加工单个微孔的时间,试验过程中激光单脉冲能量保持不变( $140 \mu\text{J}$ )。使用金相试样抛光机对加工后的铝合金板进行抛光处理,并在乙醇溶液中利用超声波清洗试样,去除铝合金板表面和微孔内的残渣。使用激光共聚焦显微镜对微孔上下表面进行表征。

图 2(c)为微孔锥度测量示意图。孔的锥度计算方法为

$$\alpha = \arctan \frac{d_1 - d_2}{2h}, \quad (1)$$

式中: $d_1$ 为微孔入口孔径; $d_2$ 为微孔出口孔径; $h$ 为微孔孔深。

### 3 结果与讨论

#### 3.1 单步法旋切打孔激光工艺参数对微孔形貌和锥度的影响

##### 3.1.1 重复频率对微孔出入口形貌及锥度的影响

激光加工参数设置如下:每层扫描次数为 100;进给次数为 20;进给量为每次  $-0.02 \text{ mm}$ (负号表示向下进给);扫描速度为  $100 \text{ mm/s}$ ;激光脉冲重复频率分别为  $5, 50, 100, 200, 300 \text{ kHz}$ 。在这些参数下研究激光脉冲重复频率对微孔出入口形貌及锥度的影响规律。

不同脉冲重复频率下,飞秒激光单步法旋切打孔工艺加工的微孔的入、出口形貌分别如图 4(a)和图 4(b)所示。图 4(c)为脉冲重复频率与出入口孔径及锥度的关系图。结果显示,随着脉冲重复频率的增加,微孔入口孔径变化很小( $226 \sim 247 \mu\text{m}$ )。与此不同的是,当脉冲重复频率从  $5 \text{ kHz}$  增加到  $50 \text{ kHz}$  时,

微孔出口的孔径从  $88 \mu\text{m}$  增加到了  $157 \mu\text{m}$ 。这是由于当脉冲重复频率为  $5 \text{ kHz}$  时,脉冲间隔时间较长( $200 \mu\text{s}$ ),前一个脉冲产生的部分能量在下一个脉冲到来之前已经通过晶格向外扩散,热量无法持续累积导致材料的去除效率较低,从而导致微孔出口孔径较小,并造成较大的锥度。当激光脉冲重复频率增加到  $50 \text{ kHz}$  时,脉冲间隔时间大幅减小( $20 \mu\text{s}$ ),通过晶格热扩散损失的能量减少,从而形成更强的热累积效应,激光脉冲引起的高温更容易达到材料的烧蚀阈值,从而扩大了微孔出口孔径,并减小了锥度。当激光重复频率高于  $50 \text{ kHz}$  时,试样下表面的激光热累积效应达到饱和,因此微孔的出口孔径几乎不发生变化。然而,由于脉冲重复频率的增加,激光平均输出功率提高,微孔入口处的热累积效应增加,因此入口孔径略有增加,微孔锥度也略有增加。

##### 3.1.2 扫描次数对微孔出入口形貌及锥度的影响

激光加工参数设置如下:脉冲重复频率为  $100 \text{ kHz}$ ;进给次数为 20;进给量为每次  $-0.02 \text{ mm}$ ;扫描速度为  $100 \text{ mm/s}$ ;激光每层扫描次数分别为 10、40、70、100、200。在这些参数下研究激光扫描次数对微孔出入口形貌和锥度的影响。不同扫描次数下,飞秒激光单步法旋切打孔工艺加工的微孔的入、出口形貌分别如图 5(a)和图 5(b)所示。图 5(c)为扫描次数与出入口孔径及锥度的关系图。结果显示,随着扫描次数的增加,微孔入口孔径几乎不发生变化( $228 \sim 232 \mu\text{m}$ )。而当扫描次数为 10 时,微孔出口孔径仅为  $96 \mu\text{m}$ ,当扫描次数为 40 时,出口孔径急剧增加到  $151 \mu\text{m}$ 。随着扫描次数的继续增加,出口孔径的变化趋缓,最后稳定在  $163 \mu\text{m}$  左右。这是因为当扫描次数较少时,由于等离子体屏蔽的影响<sup>[34]</sup>,到达微孔底部的激光能量较少,激光难以对微孔底部进行充分的加工,因此出口孔径小,锥度大。随着扫描次数的增



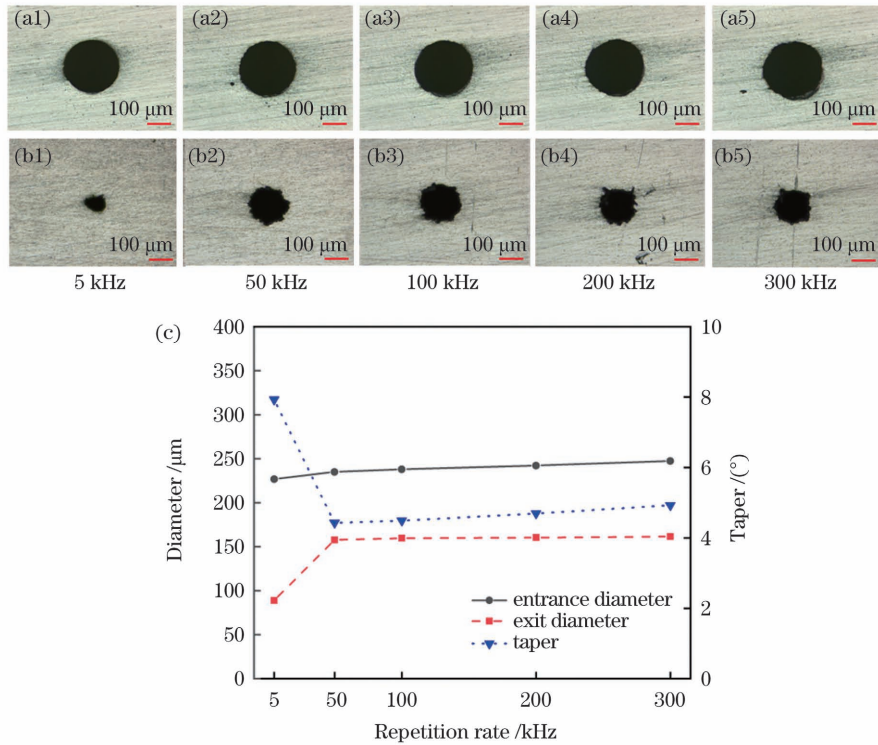


图 4 不同重复频率下单步法旋切打孔工艺加工的微孔出入口形貌及重复频率与孔径、锥度的关系图。(a1)~(a5)入口形貌；(b1)~(b5)出口形貌；(c)重复频率与孔径及锥度的关系图

Fig. 4 Entrance and exit morphologies of microholes processed by single-step trepanning drilling method under different repetition rates and influence of repetition rate on pore size and taper. (a1)–(a5) Morphologies of entrance; (b1)–(b5) morphologies of exit; (c) influence of repetition rate on pore size and taper

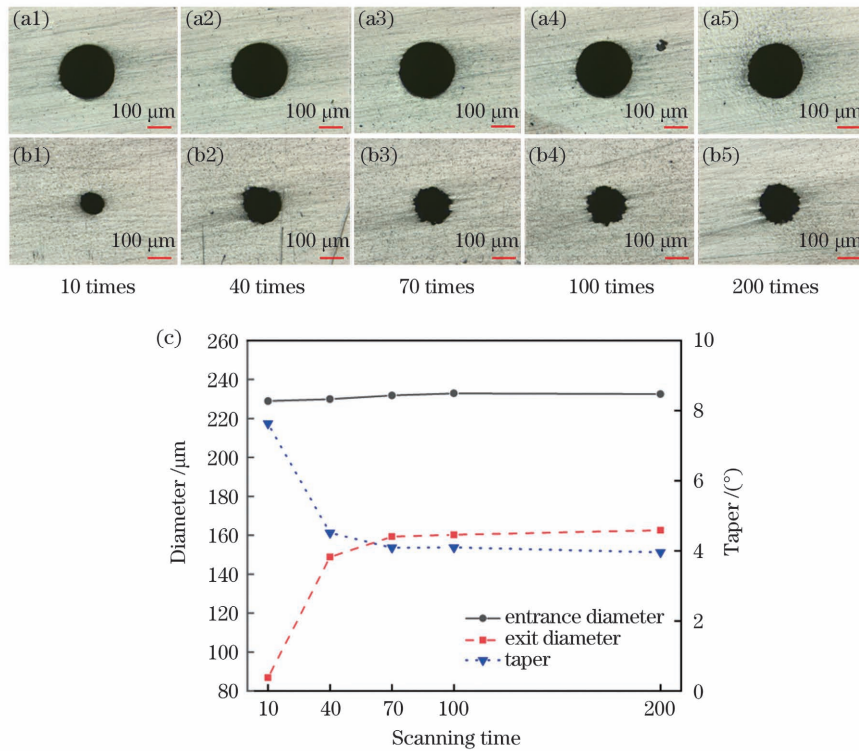


图 5 不同扫描次数下单步法旋切打孔工艺加工的微孔出入口形貌及扫描次数与孔径、锥度的关系图。(a1)~(a5)入口形貌；(b1)~(b5)出口形貌；(c)扫描次数与孔径及锥度的关系图

Fig. 5 Entrance and exit morphologies of microholes processed by single-step trepanning drilling method under different scanning times and influence of scanning time on pore size and taper. (a1)–(a5) Morphologies of entrance; (b1)–(b5) morphologies of exit; (c) influence of scanning time on pore size and taper

加,到达微孔底部的能量增加,微孔底部得到充分的加工,微孔出口孔径增大并逐渐达到加工能力的上限,出口孔径不再增加。此外,由出口形貌可以看出,多次扫描可以改善由加工不充分导致的出口圆度差的问题。

### 3.1.3 进给次数对微孔出入口形貌及锥度的影响

激光加工参数设置如下:重复频率为 100 kHz;每层扫描次数为 100;进给量为每次 0.02 mm;扫描速度为 100 mm/s;进给次数分别为 5、10、20、40、60。在这些参数下研究进给次数对微孔出入口形貌及锥度的影响,结果如图 6 所示。

随着进给次数的增加,激光焦点逐渐向下移动,出入口孔径都出现不同程度的增大。但由于激光焦点的向下移动,微孔下部的激光能量密度高于微孔上部的激光能量密度,因此微孔出口孔径的增加量大于入口孔径的增加量。由图 6(c)可以发现,经过 40 次进给后,得到的微孔的锥度最小。当进给次数达到 60 时,激光焦点位于铝合金薄板的下方,激光脉冲处于负离焦状态,再加上倾斜孔壁对激光的散射作用,微孔底部的激光能量密度急剧下降,使得入口孔径的增加量大于出口孔径的增加量,微孔锥度反而增大。

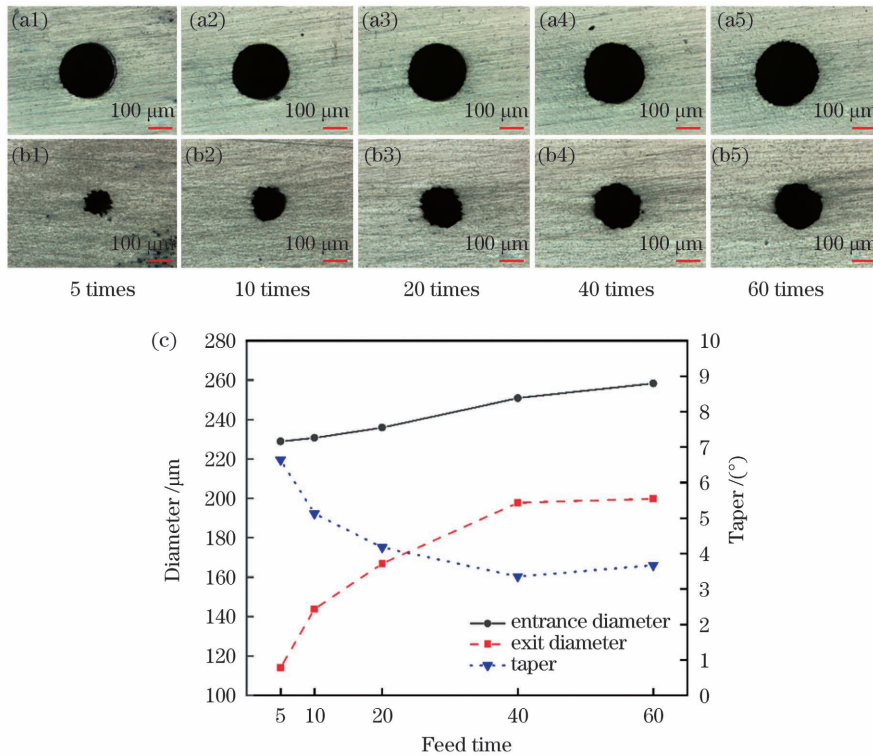


图 6 不同进给次数下单步法旋切打孔工艺加工的微孔出入口形貌及进给次数与孔径、锥度的关系图。(a1)~(a5)入口形貌;(b1)~(b5)出口形貌;(c)进给次数与孔径及锥度的关系图

Fig. 6 Entrance and exit morphologies of microholes processed by single-step trepanning drilling method under different feed times and influence of feed time on pore size and taper. (a1)~(a5) Morphologies of entrance; (b1)~(b5) morphologies of exit; (c) influence of feed time on pore size and taper

### 3.1.4 扫描速度对微孔出入口形貌及锥度的影响

激光加工参数设置如下:脉冲重复频率为 100 kHz;每层扫描次数为 100;进给次数为 20;进给量为每次 0.02 mm;激光扫描速度分别为 10, 50, 100, 200, 400 mm/s。在这些参数下研究激光扫描速度对微孔出入口形貌和锥度的影响规律,结果如图 7 所示。

微孔的出入口孔径均随着扫描速度的增加而减小,但变化速率有所不同。微孔入口孔径在扫描速度为 10~200 mm/s 时变化很小(251~245 μm),当扫描速度为 400 mm/s 时,入口孔径急剧下降到 231 μm。微孔出口孔径也随着扫描速度的增加持续减小,当扫描速度从 10 mm/s 增加到 200 mm/s 时,出口孔径呈

线性减小,当扫描速度增加到 400 mm/s 时,出口孔径急剧下降到 150 μm。出口孔径的下降速率大于入口孔径的下降速率,导致微孔锥度增大。激光扫描速度与脉冲重复频率共同决定了光斑搭接率,光斑搭接率越高,单位面积内的烧蚀时间越长,材料烧蚀加工越充分,因此微孔的出入口孔径相差越小,相应的锥度更小。光斑搭接率越小,单位面积内的烧蚀时间越少,材料烧蚀加工不充分,导致微孔出口直径变小,锥度变大。但扫描速度太小将大大影响激光加工的效率,难以满足工业生产的需要。

### 3.2 三步法旋切打孔加工工艺及加工机理研究

根据上述单步法旋切打孔的结果,本文选取合适的激光工艺参数,采用飞秒激光三步法旋切打孔

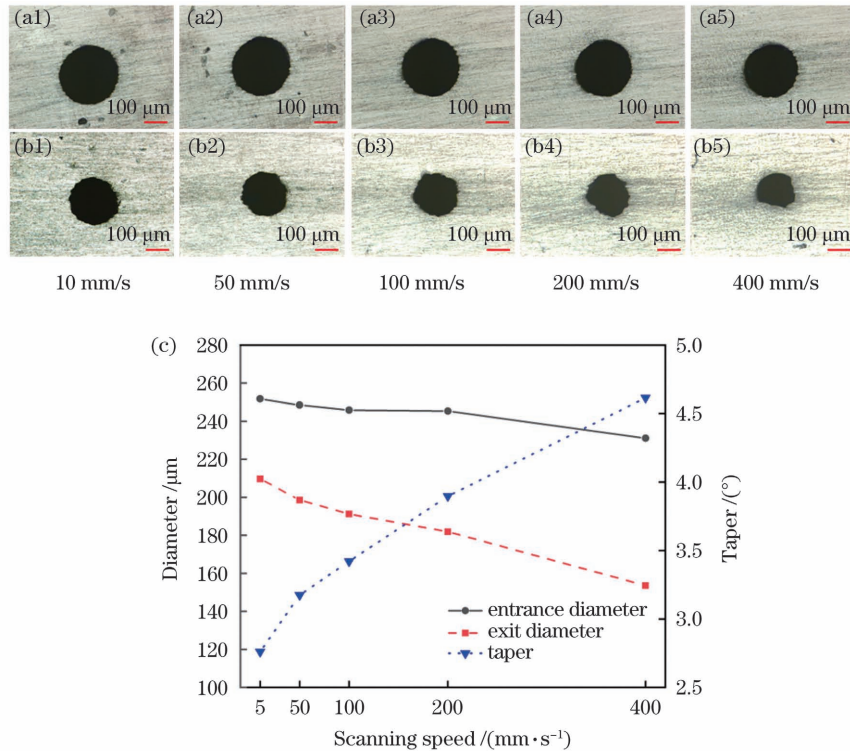


图 7 不同扫描速度下单步法旋切打孔工艺加工的微孔出入口形貌及扫描速度与孔径、锥度的关系图。(a1)~(a5)入口形貌；(b1)~(b5)出口形貌；(c)扫描速度与孔径、锥度的关系图

Fig. 7 Entrance and exit morphologies of microholes processed by single-step trepanning drilling method under different scanning speeds and influence of scanning speed on pore size and taper. (a1)~(a5) Morphologies of entrance; (b1)~(b5) morphologies of exit; (c) influence of scanning speed on pore size and taper

工艺在 1 mm 厚铝合金板上加工直径为 200 μm 的微孔，与单步法旋切打孔工艺加工的微孔的出入口形貌、锥度进行对比，并对微孔入口表面的飞溅物分布进行分析。

### 3.2.1 单步法旋切打孔工艺与三步法旋切打孔工艺加工的微孔的出入口形貌及锥度对比

激光加工参数设置如下：脉冲重复频率为 100 kHz；每层扫描次数为 100；进给量为每次 0.02 mm；扫描速度为 100 mm/s。图 8(a) 和图 8(b) 分别为使用单步法旋切打孔工艺与三步法旋切打孔工艺进给 20 次后的微孔出入口形貌，图 8(c) 和图 8(d) 分别为利用单步法旋切打孔工艺与三步法旋切打孔工艺进给 40 次后的微孔出入口形貌，图 8(e) 是对微孔出入口孔径及锥度的表征结果。

通过对比单步法旋切打孔工艺与三步法旋切打孔工艺的加工结果，可以发现，利用三步法旋切打孔工艺加工的微孔的出口孔径更大且圆度更好，微孔边缘更加光滑。利用三步法旋切打孔工艺加工的微孔的锥度明显下降，最小达到了 0.78°，比相同加工参数下单步法旋切打孔工艺加工的微孔的锥度下降了 31%。这是因为在单步法旋切打孔时，激光逐层递进扫描加工，

直至微孔底部被击穿。在此过程中，激光烧蚀加工产生的熔渣及等离子体会对后续激光脉冲产生散射干扰和等离子体屏蔽效应，从而造成微孔底部加工困难，影响出口形貌及锥度[图 8(a)]。三步法旋切打孔工艺先将材料击穿形成预制中心孔洞，然后拓宽孔径和修饰孔形，打孔过程中产生的大部分飞溅物和熔渣会通过中心孔的孔底排出，从而减少对激光束的散射干扰，使更多的激光能量用于材料的去除，改善了微孔的出口形貌，降低了微孔锥度。

三步法旋切打孔工艺特殊的加工方式需要对 Z 轴进行多次升降，这会一定程度上影响打孔效率。根据上面的研究，激光加工参数设置如下：脉冲重复频率为 100 kHz；每层扫描次数为 100；进给量为每次 0.02 mm；扫描速度为 100 mm/s；进给次数分别为 5、10、20、40、60。在这些参数下测量了单步法与三步法旋切打孔工艺加工单个微孔的时间，结果如表 3 所示。结果表明，随着进给次数的增加，三步法旋切打孔工艺的加工时间逐渐增加，但与单步法旋切打孔工艺相比，最大时间差仅为 6 s。因此，三步法旋切打孔工艺对加工效率的影响完全在可以接受的范围内。



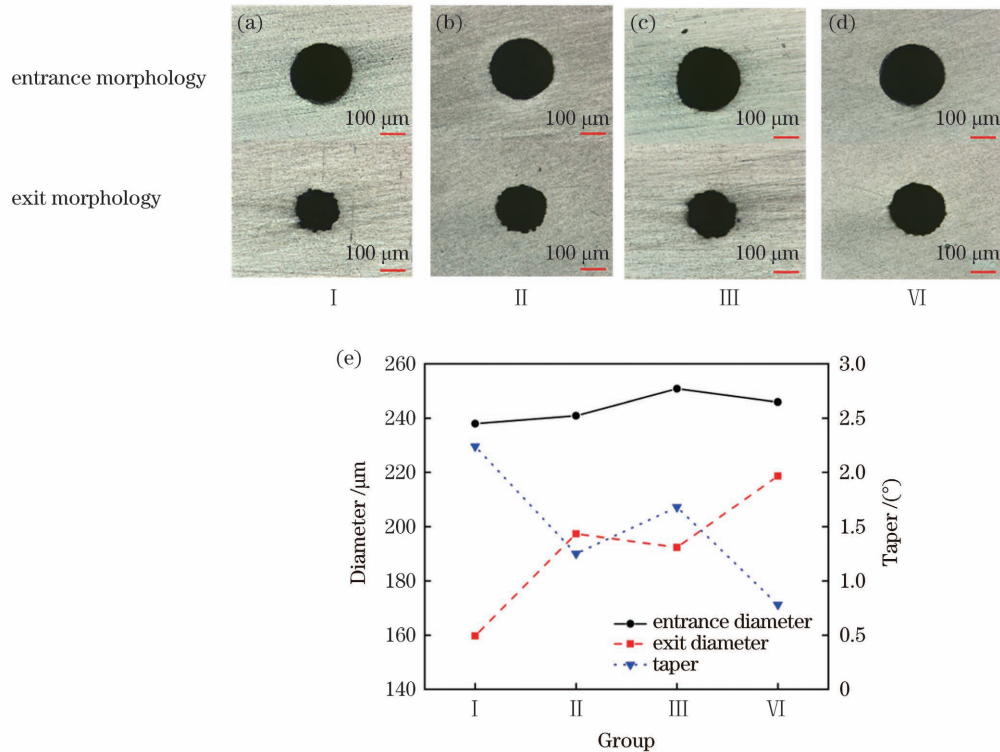


图 8 单步法旋切打孔工艺与三步法旋切打孔工艺加工的微孔的出入口形貌及孔径、锥度对比图。(a)进给 20 次,单步法旋切打孔;(b)进给 20 次,三步法旋切打孔;(c)进给 40 次,单步法旋切打孔;(d)进给 40 次,三步法旋切打孔;(e)孔径和锥度

Fig. 8 Comparison of entrance and exit morphologies, pore sizes, and tapers of microholes processed by single-step trepanning drilling method and three-step trepanning drilling method. (a) Feeding 20 times, single-step trepanning drilling; (b) feeding 20 times, three-step trepanning drilling; (c) feeding 40 times, single-step trepanning drilling; (d) feeding 40 times, three-step trepanning drilling; (e) pore size and taper

表 3 不同进给次数下单步法与三步法旋切打孔工艺加工单个微孔的时间

Table 3 Processing time of single microhole by single-step trepanning drilling method and three-step trepanning drilling method under different feeding times unit: s

Feed time	5	10	20	40	60
Single-step	16	30	58	115	172
Three-step	16	31	60	119	178

### 3.2.2 单步法旋切打孔与三步法旋切打孔中出入口处飞溅物的分析

利用第一圆环在铝合金板上预制微小孔洞,后续加工过程中产生的飞溅物和熔渣会通过孔底排出,减少了对激光束的散射干扰,这是三步法旋切打孔工艺取得良好加工效果的主要原因。本部分对比研究了两种加工方式下微孔入口处的飞溅物。激光加工参数设置如下:重复频率为 100 kHz;每层扫描次数为 100;进给次数为 40;进给量为每次  $-0.02\text{ mm}$ ;扫描速度为  $100\text{ mm/s}$ 。

采用单步法旋切打孔和三步法旋切打孔工艺加工的微孔的入口处飞溅物分析结果如图 9 所示。可以发现,在单步法旋切打孔过程中,由于绝大部分的等离子体和熔渣从微孔入口排出,因此微孔入口处堆积了大量的飞溅物,且飞溅物分布范围较大。而在三步法旋切打孔过程中,由于中心预制孔的存在,等离子体和熔渣可以从微孔出口顺利排出,因此微孔入口处的飞溅物较少,且分布范围较小。根据激光共聚焦显微镜拍摄的飞溅物 3D 分布结果可以看到,单步法旋切打孔

工艺加工的微孔的入口处飞溅物高度为  $40\ \mu\text{m}$ ,而三步法旋切打孔工艺加工的微孔的入口处飞溅物高度仅为  $17\ \mu\text{m}$ 。微孔入口处堆积的大量飞溅物不仅会堵塞孔洞,阻碍激光加工产生的熔渣和等离子体的排出,还会影响激光束的聚焦,导致加工效率低,带来微孔圆度和锥度差等问题。同时,在实际应用中,还需要通过额外的后处理工艺去除表面飞溅物,以避免对产品性能产生不良的影响,这进一步提高了生产成本。对于三步法旋切打孔工艺,影响其加工能力的关键因素是预制中心孔能否顺利形成,因此,该工艺对微孔的尺寸及材料厚度有一定的要求。本文所用激光器的光斑直径为  $30\ \mu\text{m}$ ,因此中心孔的孔径  $\geq 30\ \mu\text{m}$ 。考虑到后续的扩孔和修孔过程,建议采用三步法旋切打孔工艺时,目标微孔的孔径最好  $\geq 50\ \mu\text{m}$ 。目前,激光打孔可以实现 10:1 的深径比<sup>[33,35]</sup>,因此,当微孔直径为  $50\ \mu\text{m}$  时,材料的厚度可以达到  $500\ \mu\text{m}$ ,随着孔径的增加,材料的厚度也可以增加。但如果打孔材料太厚,会影响中心孔制备过程中等离子体的排出,导致打孔失败。

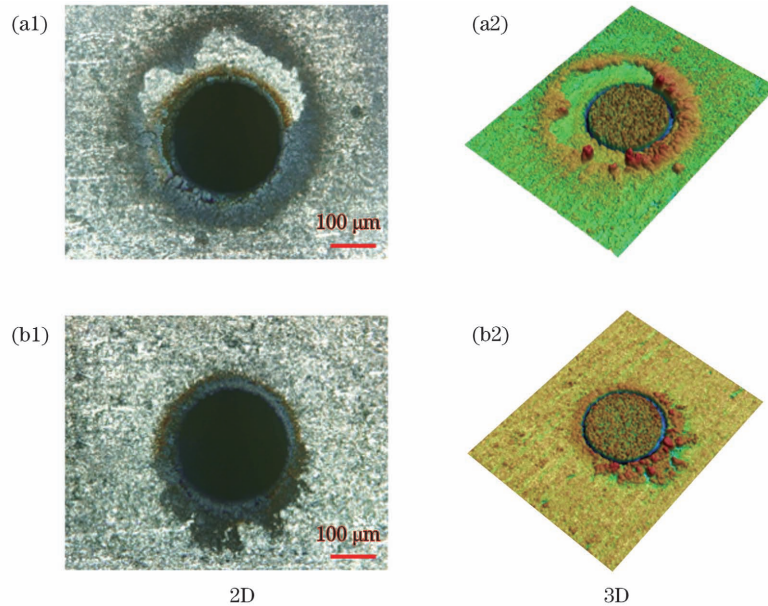


图 9 单步法旋切打孔与三步法旋切打孔工艺加工的微孔的入口处飞溅物。(a1)(a2)单步法旋切打孔;(b1)(b2)三步法旋切打孔  
Fig. 9 Spatters at entrances of microholes processed by single-step trepanning drilling method and three-step trepanning drilling method. (a1)(a2) Single-step trepanning drilling; (b1)(b2) three-step trepanning drilling

## 4 结 论

针对铝合金材料激光打孔出入口形貌差、锥度大等问题,采用控制变量法研究了旋切打孔中激光重复频率、扫描次数、扫描速度及进给次数对微孔出入口形貌和锥度的影响规律。在单步法旋切打孔工艺中,激光的进给次数和扫描速度对微孔出口孔径和出口形貌的影响最大。随着进给次数的增加,微孔下部的激光能量密度高于微孔上部的激光能量密度,因此微孔出口孔径的增加量大于入口孔径的增加量。过多的进给次数会使激光脉冲处于负离焦状态,使入口孔径的增加量大于出口孔径的增加量,微孔锥度反而增大。相对较小的扫描速度可以提高微孔的出口圆度,并减小孔锥度,但过小的扫描速度会导致加工时间过长,不利于实际生产应用。激光重复频率和扫描次数对微孔形貌和锥度的影响较小,当脉冲重复频率较低时,激光热量无法持续累积,导致材料的去除效率低,从而微孔出口孔径较小,造成较大的锥度。随着激光脉冲重复频率的增加,热累积效应增强,从而扩大了微孔的出口孔径,减小了锥度。当激光重复频率高于 50 kHz 时,微孔下部的激光热累积效应达到饱和,因此微孔的出口孔径几乎不发生变化。然而,由于脉冲重复频率的增加,激光平均输出功率增加,微孔入口更容易受到热累积效应的影响,此时入口孔径略有增加,微孔锥度增加。

为了进一步减小微孔锥度,改善微孔出入口形貌,提出了三步法旋切打孔工艺。与单步法旋切打孔工艺的加工结果对比,可以发现:1) 在相同的激光工艺参数下,三步法旋切打孔工艺可以明显改善微孔出入口形貌,降低微孔锥度。采用三步法旋切打孔工艺,微孔锥度最小为  $0.78^\circ$ ,比相同条件下单步法旋切打孔工艺加

工的微孔的锥度减小了 31%,且三步法旋切打孔工艺对加工效率的影响很小。2) 在三步法旋切打孔过程中,产生的飞溅物体积减小且扩散面积减小,飞溅物的堆积高度明显下降。这是由于预制中心孔的存在,大部分飞溅物由孔底排出,从而极大减少了入口处堆积的飞溅物。

## 参 考 文 献

- [1] Yang L, Kan R, Ren J, et al. Effect of film cooling arrangement on impingement heat transfer on turbine blade leading edge [C] // Proceedings of ASME Turbo Expo 2013: Turbine Technical Conference and Exposition, June 3-7, 2013, San Antonio, Texas, USA. New York: Amer SOC Mechanical Engineers, 2013.
- [2] Sundaram N, Thole K A. Film-cooling flowfields with trepanned holes on an endwall[J]. Journal of Turbomachinery, 2009, 131(4): 041007.
- [3] Lee K D, Choi D W, Kim K Y. Optimization of ejection angles of double-jet film-cooling holes using RBNN model [J]. International Journal of Thermal Sciences, 2013, 73: 69-78.
- [4] 魏明锐, 文华, 刘会猛, 等. 柴油机孔式喷油嘴内空穴流动的模拟分析[J]. 内燃机学报, 2006, 24(6): 526-530.
- [5] Wei M R, Wen H, Liu H M, et al. Simulation analysis on cavitation flow in a diesel engine nozzle [J]. Transactions of CSICE, 2006, 24(6): 526-530.
- [5] Xia J, Zhang Q K, Huang Z, et al. Experimental study of injection characteristics under diesel's sub/trans/supercritical conditions with various nozzle diameters and injection pressures [J]. Energy Conversion and Management, 2020, 215: 112949.
- [6] 朱帅杰, 张朝阳, 储松林, 等. 海量微孔水辅助法皮秒激光加工技术的研究及应用[J]. 中国激光, 2020, 47(3): 0302002.
- [6] Zhu S J, Zhang Z Y, Chu S L, et al. Research and application of massive micropores water-assisted picosecond laser processing technology [J]. Chinese Journal of Lasers, 2020, 47(3): 0302002.
- [7] 熊厚. 纳秒激光薄铝板精密打孔研究[D]. 武汉: 湖北工业大学, 2016: 2.
- [7] Xiong H. Nanosecond laser drilling of thin aluminum sheets [D]. Wuhan: Hubei University of Technology, 2016: 2.
- [8] Cobo P, de Espinosa F M. Proposal of cheap microporated panel absorbers manufactured by infiltration [J]. Applied



- Acoustics, 2013, 74(9): 1069-1075.
- [9] Su M N, Young B. Material properties of normal and high strength aluminium alloys at elevated temperatures [J]. Thin-Walled Structures, 2019, 137: 463-471.
- [10] Donald L. Erich, 李行健. 机械合金化铝合金的优点 [J]. 轻金属, 1983(6): 55-57.  
Erich D L, Li X J. Advantages of mechanized aluminum alloy [J]. Light Metals, 1983(6): 55-57.
- [11] Hirsch J. Aluminium in innovative light-weight car design [J]. Materials Transactions, 2011, 52(5): 818-824.
- [12] 隋育栋, 王渠东. 铸造耐热铝合金在发动机上的应用研究与发展 [J]. 材料导报, 2015, 29(3): 14-19.  
Sui Y D, Wang Q D. Development of heat-resistant cast aluminum alloy for engine applications [J]. Materials Review, 2015, 29(3): 14-19.
- [13] von Zengen K H. Aluminium in future cars-a challenge for materials science [J]. Materials Science Forum, 2006, 519/520/521: 1201-1208.
- [14] Hirsch J. Recent development in aluminium for automotive applications [J]. Transactions of Nonferrous Metals Society of China, 2014, 24(7): 1995-2002.
- [15] Heinz A, Haszler A, Keidel C, et al. Recent development in aluminium alloys for aerospace applications [J]. Materials Science and Engineering: A, 2000, 280(1): 102-107.
- [16] Vermeulen B, van Tooren M J L. Design case study for a comparative performance analysis of aerospace materials [J]. Materials & Design, 2006, 27(1): 10-20.
- [17] Vasudevan S, Lakshmi J, Jayaraj J, et al. Remediation of phosphate-contaminated water by electrocoagulation with aluminium, aluminium alloy and mild steel anodes [J]. Journal of Hazardous Materials, 2009, 164(2/3): 1480-1486.
- [18] Sundararajan M, Devarajan M, Jaafar M. Investigation of surface and mechanical properties of anodic aluminium oxide (AAO) developed on Al substrate for an electronic package enclosure [J]. Surface and Coatings Technology, 2020, 401(12): 126273.
- [19] Hu F Q, Song B Y, Bai J C, et al. Micro-EDM for an aluminium matrix composite [J]. Key Engineering Materials, 2010, 447/448: 233-237.
- [20] Bauer J, Frost F, Lehmann A, et al. Finishing of metal optics by ion beam technologies [J]. Optical Engineering, 2019, 58(9): 092612.
- [21] 阿占文, 陈灵灵, 吴影, 等. 超快激光旋光钻孔孔径和锥度的控制 [J]. 中国激光, 2021, 48(8): 0802017.  
A Z W, Chen L L, Wu Y, et al. Controlling of diameter and taper in ultrafast laser helical drilling [J]. Chinese Journal of Lasers, 2021, 48(8): 0802017.
- [22] 郭敏超, 王明娣, 张胜江, 等. FR-4 覆铜板飞秒激光微孔加工工艺研究 [J]. 中国激光, 2020, 47(12): 1202008.  
Guo M C, Wang M D, Zhang S J, et al. Techniques for femtosecond laser processing of micro-holes in FR-4 copper clad laminate [J]. Chinese Journal of Lasers, 2020, 47(12): 1202008.
- [23] 张学谦, 邢松龄, 刘磊, 等. 带热障涂层的高温合金飞秒激光旋切打孔 [J]. 中国激光, 2017, 44(1): 0102013.  
Zhang X Q, Xing S L, Liu L, et al. Trepanning of super-alloy with thermal barrier coating using femtosecond laser [J]. Chinese Journal of Lasers, 2017, 44(1): 0102013.
- [24] 刘晓东, 陈亮, 王曦照, 等. 皮秒激光旋切制孔工艺研究 [J]. 激光与光电子学进展, 2022, 59(7): 0102013.  
Liu X D, Chen L, Wang X Z, et al. Study on technology of picosecond laser making micro-hole with helical drilling [J]. Laser & Optoelectronics Progress, 2022, 59(7): 0102013.
- [25] 邓树森. 激光加工技术及其应用 [J]. 物理, 1995, 24(2): 99-102, 119.  
Deng S S. Laser processing technology and its application [J]. Physics, 1995, 24(2): 99-102, 119.
- [26] Richardson M. Laser materials processing technologies and the future [C]//2015 11th Conference on Lasers and Electro-Optics Pacific Rim (CLEO-PR), August 24-28, 2015, Busan, Korea (South). New York: IEEE Press, 2015.
- [27] Pierron N, Sallamand P, Jouvard J M, et al. Determination of an empirical law of aluminium and magnesium alloys absorption coefficient during Nd: YAG laser interaction [J]. Journal of Physics D: Applied Physics, 2007, 40(7): 2096-2101.
- [28] Tunna L, O'Neill W, Khan A, et al. Analysis of laser micro drilled holes through aluminium for micro-manufacturing applications [J]. Optics and Lasers in Engineering, 2005, 43(9): 937-950.
- [29] Sercombe T B, Li X. Selective laser melting of aluminium and aluminium metal matrix composites: review [J]. Materials Technology, 2016: 1-9.
- [30] Krstulović N, Shannon S, Stefanuik R, et al. Underwater-laser drilling of aluminum [J]. The International Journal of Advanced Manufacturing Technology, 2013, 69(5): 1765-1773.
- [31] 钱晓忠, 夏凯波, 任乃飞. 铝合金脉冲激光打孔成形质量规律研究 [J]. 应用激光, 2016, 36(6): 728-734.  
Qian X Z, Xia K B, Ren N F. Investigation on microhole formation quality law for pulsed laser drilling of aluminum alloy [J]. Applied Laser, 2016, 36(6): 728-734.
- [32] Ahn D G, Jung G W. Influence of process parameters on drilling characteristics of Al<sub>1050</sub> sheet with thickness of 0.2 mm using pulsed Nd: YAG laser [J]. Transactions of Nonferrous Metals Society of China, 2009, 19: s157-s163.
- [33] Zhao W Q, Liu H D, Shen X W, et al. Percussion drilling hole in Cu, Al, Ti, and Ni alloys using ultra-short pulsed laser ablation [J]. Materials, 2019, 13(1): 31.
- [34] Ho C C, Tseng G R, Chang Y J, et al. Laser percussion drilling of highly reflective metals with external interdigital electrodes [J]. Precision Engineering, 2016, 43: 43-51.
- [35] Wang M L, Yang L J, Zhang S, et al. Experimental investigation on the spiral trepanning of K24 superalloy with femtosecond laser [J]. Optics & Laser Technology, 2018, 101: 284-290.

## Femtosecond Laser Single-step and Three-step Trepanning Drilling Technology of Aluminum Alloy

Ren Yunpeng<sup>1\*</sup>, Cheng Li<sup>1</sup>, Zhou Wangfan<sup>1</sup>, Chen Yan<sup>2</sup>, He Kun<sup>1</sup>, Tu Xincheng<sup>1</sup>,  
Ye Yunxia<sup>1</sup>, Ren Naifei<sup>1</sup>

<sup>1</sup> School of Mechanical Engineering, Jiangsu University, Zhenjiang 212013, Jiangsu, China;

<sup>2</sup> School of Materials Science and Engineering, Jiangsu University, Zhenjiang 212013, Jiangsu, China

### Abstract

**Objective** With the rapid development of modern industry, aluminum alloy has been widely used in industrial production due to its excellent physical and chemical properties. Meanwhile, the preparation of high-quality microholes in aluminum

alloys is in high demand. Laser drilling technology, when compared with other traditional microhole machining techniques, has the advantages of high processing accuracy and efficiency, good flexibility, and no tool loss. However, the high reflectivity and thermal conductivity of aluminum alloys make it challenging to prepare high-quality microholes. Hence, it is crucial to study the influence of laser parameters on microhole morphologies and tapers and develop laser drilling technology for microholes in aluminum alloys.

**Methods** In this study, we use a femtosecond laser to drill microholes with a diameter of  $200\ \mu\text{m}$  in a 1 mm thick 1060 aluminum alloy. First, the influence of the laser repetition rate, scanning time, scanning speed, and feed time on microhole morphologies and tapers is studied using the control variable method. Then, based on the single-step trepanning drilling method [Fig. 2 (a)], a three-step trepanning drilling method [Fig. 2 (b)] is proposed to solve the problems of big taper and poor entrance and exit morphologies. The three circles are set as one ring in the three-step trepanning drilling method. The innermost circle (C1) is first scanned clockwise, and the laser moves toward the first ring's outer circle (C3). After the first layer scanning, the laser feeds down a distance and the above process of C1–C3 is repeated until the center perforated hole forms. Subsequently, the laser is focused on the C4–C9 circles to complete the second and third rings similarly and finally the microhole processing is finished. In the three-step trepanning drilling, the drilling process is divided into three steps: the first ring is used to form the center microhole, the second ring is used to widen it, and the third ring is used to improve the hole morphology [Fig. 3 (b)]. The entrance and exit morphologies and the surface slag of microholes are analyzed using a laser confocal microscope. The corresponding tapers are calculated.

**Results and Discussions** The influence of laser repetition rate, scanning time, scanning speed, and feed time on microhole morphologies and tapers using the single-step trepanning drilling method is analyzed. According to the results, the low repetition rate makes the heat accumulation unsustainable, which causes low material removal efficiency and a large taper. The heat accumulation at the lower part of the microhole reaches saturation when the repetition rate is increased to 50 kHz, and the microhole taper is the smallest (Fig. 4). Scanning time has a similar effect as feeding time on the taper and entrance and exit morphologies of the microhole. Multiple scans can improve the roundness of the outlet (Fig. 5). With the increase in feed times, the laser energy density in the lower part of the microhole exceeds that in the upper part of the microhole, so the microhole exit diameter increases faster than the entrance diameter. Too many feed times will increase taper (Fig. 6). The laser scanning speed and repetition rate determine the spot overlap ratio; the higher the spot overlap ratio, the more material is ablated and the smaller the taper (Fig. 7). Based on the above research results, the appropriate laser parameters are selected for the comparative experiment of single-step and three-step trepanning drilling methods. The morphologies and tapers of microholes processed by three-step trepanning drilling method are greatly improved (Fig. 8). This is because, in the single-step drilling process, the slag and plasma generated by laser ablation will cause interference and plasma shielding effect on the subsequent laser pulse, making processing the lower part of the microhole difficult and affecting the exit morphology and taper. However, most slag and plasma produced in the three-step drilling process will be discharged through the bottom of the center hole, which reduces scattering interference to the laser beam. Therefore, the morphologies of the microholes will be improved, and the tapers will be reduced. Observations of slag on the surface of the microhole processed by two methods support this analysis (Fig. 9). Although the three-step trepanning drilling method requires multiple feeds, it has little influence on processing time and efficiency (Table 1).

**Conclusions** In this study, the influence of laser repetition rate, scanning time, scanning speed, and feed time on microhole morphologies and tapers is studied using the control variable method. A three-step trepanning drilling method is proposed to solve the problems of a big taper and poor morphology caused by single-step trepanning drilling. The morphologies and tapers of the microholes prepared by the three-step trepanning drilling method are improved. The minimum taper is  $0.78^\circ$ , which is 31% lower than those of the microholes prepared by single-step trepanning drilling method with the same laser parameters. The main reason is that the three-step trepanning drilling method can effectively promote the discharge of slag and plasma in the drilling process, which reduces disturbance to laser energy and hence improves the stability and uniformity of laser energy.

**Key words** laser technique; femtosecond laser; trepanning drilling; aluminum alloy; taper